JOURNAL OF APPLIED ELECTROCHEMISTRY 6 (1976) 485–505

Macrokinetics of processes in hydrogen–oxygen fuel cells and electrolysers

L. M. PISMEN*, YU. M. VOLFKOVICH, V. S. BAGOTZKY

Institute of Electrochemistry of the Academy of Sciences of the USSR

Received 10 November 1975

A theory of the macrokinetics of electrode reactions in gas–liquid electrodes has been developed for the case of electrochemical reactions occurring at the electrodes of an hydrogen–oxygen fuel cell or of a water electrolyser. This theory takes account of the convective flows arising at electrodes of this type due to electrochemical reactions, which exert strong influences on transport phenomena.

The concepts developed have been used for calculations of the large-scale macrokinetics in hydrogen–oxygen fuel cells and electrolysers with capillary membranes, which include mass transfer processes in the electrodes, the capillary membrane and in the boundary gas layers adjoining the electrode, as well as the flooding and drying of porous electrodes due to changes in the working conditions. Account is also taken of the self-regulation of the supply and removal of water vapour.

List of symbols

C = total concentration, mol cm^{-3}
c = solute concentration mol cm^{-3}
c_w = solvent concentration, mol cm^{-3}
D = effective diffusivity, cm^2 s^{-1}
E = e.m.f., V
F = Faraday constant, C mol^{-1}
f_c = dp_w/dc, see Equation 6
I = current density (total), A cm^{-2}
$i(x)$ = current density at cross-section x, A cm^{-2}
J = mass flux, mol cm^{-2} s^{-1}
K = permeability, cm^2
k = rate constant, s^{-1}
l = electrode thickness, cm
M = molecular weight, g mol^{-1}
p = gas-phase concentration, mol cm^{-3}
Q = rate of reaction per unit volume of porous electrode, mol cm^{-3} s^{-1}
q = rate of evaporation per unit volume, mol cm^{-3} s^{-1}
R = gas constant, erg mol^{-1} °K^{-1}
T = temperature
t = transference number
u = gas filtration velocity, cm s^{-1}
v = liquid filtration velocity, cm s^{-1}
V = voltage, V
x = co-ordinate, cm

Greek

α = dimensionless water flux through membrane (scale I/F)
β = mass transfer coefficient, cm s^{-1}
γ = see Equation 64
δ = electrode or membrane thickness, cm
ϵ = diffusion retardation factor in porous body
θ = wetting angle
μ = dynamic viscosity, g cm^{-1} s^{-1}
ν = stoichiometric coefficient ($\nu > 0$ for products and $\nu < 0$ for reactants)
Π = pressure, g cm^{-1} s^{-2}
Π_c = capillary pressure, g cm^{-1} s^{-2}
ρ = density, g cm^{-3}
σ = surface tension, g s^{-2}
χ = $t^+ c_w/c$
Φ = functions, Equation 52
ϕ = dimensionless potential (scale RT/F)
ω = liquid content

Subscripts and superscripts

g = gas reactant; gas phase
l = liquid phase (electrolyte)

* Present Address: Technion – Israel Institute of Technology, Department of Chemical Engineering, Haifa, Israel

w = solvent (water)
+ = cation
− = anion
0 = membrane
1 = hydrogen electrode
2 = oxygen electrode

1. Introduction

Most important electrochemical processes involving gaseous reactants or yielding gaseous products (for instance, current generation or electrolysis on porous electrodes) take place in porous media partially filled with electrolyte and partially with gas.

Three major factors affecting the rates of these processes are:

(1) kinetics of surface electrochemical reaction;

(2) 'microscopic' transfer processes of dissolved gases to metal/electrolyte interfaces and

(3) 'macroscopic', or large-scale transfer processes of gas and liquid reactants in the porous electrodes.

While much attention has been paid to the first two problems [1], the essential features of large-scale transfer processes were overlooked until recently [2–5], and the particular importance of convective flows in gas–liquid electrodes was slow to be recognized.

In this paper we shall concentrate on problems of 'macroscopic' transport in gas–liquid electrodes. Both microscopic stages will be accounted for by an effective kinetic function influenced both by surface kinetics and diffusion of gas reactants from gas-filled pores to the active surface. In Section 2, we give a qualitative analysis of the various factors influencing the transfer processes in a two-phase medium. The results will be applied in the subsequent sections to calculate the performance of the hydrogen–oxygen fuel cell with a capillary membrane.

2. Mass transfer in a gas–liquid porous electrode

2.1. *Transfer equations in liquid and gas phases*

Consider a system consisting of a binary electrolyte (for example, alkali solution) and a binary gas mixture containing solvent (water) vapour and an active component (hydrogen or oxygen) which upon dissolution enters into electrochemical reaction either with the anion (hydroxyl) producing water or, on the contrary, with water producing the anion. (The components given in brackets correspond to the hydrogen–oxygen fuel cell in an alkaline solution; however, the equations given below are equally valid for other processes with the same scheme; absorption of gas can be replaced by its electrochemical evolution as in the case of water electrolysis).

Suppose that both gas- and liquid-filled pores are linked into connected networks spreading throughout the porous body, so that two continuous fluid phases coexist within the pore space. Suppose also that all macroscopic variables do not change appreciably over distances comparable with the inhomogeneity scale of a porous body. Then macroscopic quasihomogeneous equations with effective transport coefficients can be written for both fluid phases.

Ion transfer equations in the electrolyte accounting for molecular diffusion, convection, migration and electrochemical reaction are of the forms

$$J^+ \equiv -D^+\frac{\mathrm{d}c}{\mathrm{d}x} + vc - D^+c\frac{\mathrm{d}\phi}{\mathrm{d}x} = 0 \qquad (1)$$

$$\frac{\mathrm{d}J^-}{\mathrm{d}x} \equiv \frac{\mathrm{d}}{\mathrm{d}x}\left(-D^-\frac{\mathrm{d}c}{\mathrm{d}x} + vc + D^-c\frac{\mathrm{d}\phi}{\mathrm{d}x}\right) = \nu_- Q. \quad (2)$$

Equations 1 and 2 take into account the electric neutrality condition so that they give both the concentration and the electrolyte potential. The Einstein relation $D^i = u^iRT/F$ between the mobility u^i and the diffusion coefficient D^i of the ith ion was also used to derive these equations. Of course, this relation is not quite correct for concentrated solutions*. But even then the transfer equations can be written in the forms (1) and (2) with additional concentration-dependent factors included in the migration terms. Since these equations include convective terms, it is more convenient to use concentrations rather than the activities even for concentrated solutions. More exact forms of transport equations would involve multicomponent diffusion coefficients

*The Einstein relation for concentrated solutions has the form: $D^i = u^i(1 + k)RT/Fz^i$, where $k = \mathrm{d}\ln f_a/\mathrm{d}\ln c$ and f_a is the activity coefficient, z^i is the charge of the ion i. For the sake of simplicity we assumed $k = 0$.

D^{ij} which are never obtained by the usual measurements, so the use of the Fick law with the empirical concentration-dependent one-component diffusion coefficients D^i appears to be the only practical choice. It should be further noticed that the effective diffusivities in Equations 1 and 2 are complicated quantities depending on the structure of the porous material and the fraction of the pores filled by electrolyte. These structural factors also influence the effective kinetic function $Q(\phi, c, p_g)$.

The choice of the flow rate in multicomponent concentrated solutions, is, in general, not unique and must correspond to the reference frame of the empirical diffusion coefficients. The solvent flow rate produced by its evolution or absorption during electrochemical reaction and evaporation–condensation processes, can be advantageously taken as the flow velocity. Such a choice is justified by the fact that convective effects due to the transport of reacting ions are taken into account in the standard method of determining the effective diffusion coefficients by measuring the electric conductivity [6]. Then the solvent balance gives the equation for the flow rate

$$\frac{d(vc_w)}{dx} = \nu_w Q - q. \tag{3}$$

The terms on the right-hand side of Equation 3 express the change of the solvent flow $J_w = vc_w$ due to electrochemical reaction and evaporation. The concentration of solvent c_w is connected with the solute concentration c and the solution density ρ by the relationship $c_w = (\rho - cM_s)/M_w$.

The transfer equations in the gas phase take the forms

$$\frac{d}{dx}\left(up_g - D_g\frac{dp_g}{dx}\right) = \nu_g Q \tag{4}$$

$$\frac{d}{dx}\left(up_w - D_g\frac{dp_w}{dx}\right) = q. \tag{5}$$

Due to the large gas–liquid interface area in a porous body, the processes of solvent vaporization and condensation proceed at a fast rate so that the distribution of solvent between two phases must be close to the equilibrium one. Therefore the transfer equations in the liquid and gas phases are conjugated by the relation between the vapour and electrolyte concentrations:

$$p_w = f(c). \tag{6}$$

So far we have obtained six equations with seven unknown variables: solute concentration c, potential ϕ, gas-phase concentrations p_g and p_w, rate of evaporation q and velocities in both phases v and u. These equations include one more variable in an implicit form, namely, the fraction of pores filled by the electrolyte, or liquid content, ω, which determines both the values of the effective diffusion coefficients and the rate of the electrochemical reaction (there is no explicit dependence of ω in the equations since all fluxes are calculated for the total cross-section of the electrode). Two remaining variables, the pressure in the gas phase $\Pi_g = (p_g + p_w)RT$ and the liquid content ω, which is directly related to the capillary pressure in the porous medium are found from the filtration equations in the liquid and in the gas (Darcy equations):

$$v = -\frac{K_l}{\mu_l}\frac{d\Pi_l}{dx} \tag{7}$$

$$u = -\frac{K_g}{\mu_g}\frac{d\Pi_g}{dx}. \tag{8}$$

Pressures in both phases are related by the condition of capillary equilibrium

$$\Pi_g - \Pi_l = \Pi_c = \frac{2\sigma\cos\theta}{r_c} \tag{9}$$

where r_c is the meniscus radius at the interface. Hence, the value of Π_c depends on the pore filling by electrolyte in a given cross-section of the electrode. In the simplest case, when the hysteresis during filling of pores by the electrolyte can be neglected, ω is expressed by the integral over the distribution function of pore radii $\psi(r)$

$$\omega = \int_{r_{min}}^{r_c} \psi(r)\,dr.$$

As will be shown below, under certain conditions the system of equations used for calculations can be considerably simplified. In particular, there is no need to consider the hydrodynamic filtration equations for ordinary electrochemical processes.

2.2. *Constant pore filling condition*

Convective flows are produced in both phases only under the action of the current taken from or passing through the electrode. Using a given current density I (calculated for the total cross-section of the electrode) and total molar concentrations in both phases, C_g, C_l, we can evaluate characteristic liquid and gas velocities

$$v \sim I/FC_l \quad u \sim I/FC_g. \tag{10}$$

Taking into account Equation 10 we obtain from Equations 7–9 the estimates for the pressure drops in both phases:

$$\Delta\Pi_g \sim \frac{Il}{FC_g}\frac{\mu_g}{K_g}; \quad \Delta\Pi_l \sim \frac{Il}{FC_l}\frac{\mu_l}{K_l}. \tag{11}$$

If the permeabilities of both phases K_g, K_l are of the same order of magnitude, the ratio of the pressure drops in the gaseous and liquid phases is equal to $\Delta\Pi_g/\Delta\Pi_l = (\mu_g/\mu_l)/(C_g/C_l)$. Within an order of magnitude, this ratio is equal to the ratio of the kinematic viscosities of both phases and, since $\nu_g \sim 10^{-1}$, $\nu_l \sim 10^{-2}$ cm^2 s^{-1}, the pressure drop in the gas phase is higher than that in the liquid.

Using Equations 7 and 9, we can estimate the maximum flow velocity in the liquid phase which could be produced in the electrode with thickness l under the action of capillary forces:

$$v_c = \frac{K_l}{\mu_l}\frac{\sigma}{l}\left(\frac{1}{r_{min}} - \frac{1}{r_{max}}\right) \sim \frac{ar_{max}^2\sigma}{\mu r_{min} l} \tag{12}$$

Here we assume that the permeability is proportional to the squared radius of the large pores through which most of the liquid inflow proceeds, with the proportionality coefficient a. Assuming $r_{max} = 10^{-5}$ cm, $r_{min} = 10^{-6}$ cm, $\mu = 10^{-2}$ g cm^{-1} s^{-1}, $\sigma = 10^2$ g s^{-2}, $a = 10^{-2}$ (this corresponds to the usual Poiseuille flow in capillaries with correction for capillary tortuosity) and $l = 10^{-2}$ cm, we obtain $v_c = 1$ cm s^{-1}. This value is much higher than the velocities which can be developed with usual currents. Assuming $C_l = 5 \times 10^{-2}$ mol cm^{-3} and $I = 0.5$ A cm^{-2} in Equation 10, we obtain $v = 10^{-4}$ cm s^{-1}. Thus, even for such a high current density we have $v \ll v_c$. Since $v \ll v_c$, the capillary pressure is practically constant throughout the electrode. If the distribution of pore radii is sufficiently wide, constancy of capillary pressure means, at the same time, constancy of pore filling by the electrolyte. The opposite limiting case $v \gg v_c$ corresponds to the regime of non-uniform liquid content when one part of the electrode is dried while another is flooded. Besides increased current density, this unfavourable regime may be also induced by use of fine-porous materials with low permeability or electrodes with narrow distributions of pore radii. On the contrary, the use of materials, containing pores of unequal widths, including wide pores which aid the liquid flow, promotes the uniform filling of the electrode by the electrolyte.

When the inequality $v \gg v_c$ holds, Equation 7 can be dropped. Then the liquid content ω is included in the system of equations as a parameter and, as it is constant throughout the electrode, can be found from integral relationships (see Section 4).

With $v \ll v_c$, gas pressure drop is not sufficient to shift appreciably the capillary equilibrium in a gas–liquid electrode, but it can still affect the transport of gaseous reactants. However, estimates based on Equation 12 show that in porous materials containing sufficiently wide pores with $r \gtrsim 10^{-5}$ cm operating out of the Knudsen diffusion region, $\Delta\Pi_g$ is small compared with the total gas pressure. Under these conditions Equation 8 can be replaced by the equation

$$p_w + p_g = C_g = \text{const}. \tag{13}$$

2.3. *Constant concentration condition*

Electrochemical reaction induces concentration gradients in both phases; on the contrary, diffusion tends to minimize these gradients. If there were no mass exchange between gas and electrolyte, concentration drops in both phases could be estimated as

$$|\Delta p_w| \sim |\Delta p_g| \sim \frac{Il}{FD_g}, \quad |\Delta c_w| \sim |\Delta c| \sim \frac{Il}{FD_l}, \tag{14}$$

$$\left|\frac{\Delta p_g}{p_g}\Big/\frac{\Delta c}{c}\right| \sim \frac{D_g p_g}{D_l c}.$$

In the hydrogen electrode $p_g/c \sim 10^{-3}$, while $D_g/D_l \sim 10^5$, and thus the gas-phase concentration drop should be much less than the liquid-phase one. With the current density $10^{-1} < I < 1$ A cm^{-2} and $l \sim 10^{-2}$ cm, considerable concentration gradients could be expected in the liquid electrolyte, but the gas-phase concentration profile must be smoothed out due to intensive diffusion. Such a discrepancy is in evident contradiction with the conditions of the solvent vaporization/condensation equilibrium. Moreover, in the hydrogen electrode even the signs of the concentration gradients imposed by diffusional fluxes in the gas and electrolyte are opposite. Which concentration distribution pattern will be actually realized, depends on the comparative efficiency of gas and liquid diffusion. Since the former is much more intensive, the uniform gas-phase composition cannot be influenced by the gradient of the solute concentration. On the contrary, the electrolyte composition will become more uniform due to the solvent evaporation in the low-concentration regions, vapour diffusion through the gas phase and condensation in the high-concentration regions. The vapour flux induced by the solute concentration gradient dc/dx equals $D_g(\partial p_w/\partial c)(dc/dx)$, and if $(D_g/D_l)(\partial p_w/\partial c) \gg 1$, the amount of vapour transferred is sufficient to smooth out the non-uniformity of the electrolyte composition. This inequality holds under the usual temperature and concentration conditions of fuel cell operations $90 < T < 100°C$, $c \sim 10\,mol\,l^{-1}$.

In the oxygen electrode, due to the lower value of the gas diffusivity, equalizing of the electrolyte concentration by vapour transport is less effective, but even there, uniform electrolyte composition can be anticipated at current densities around 10^{-1} A cm^{-2}. Considerable concentration gradients can be created when current and liquid content are increased or temperature lowered. Numerical calculations confirm that concentration gradients in the electrodes are negligible at moderate current densities (see Section 4). The important role of transfer processes in the gas phase in gas–liquid porous electrodes was recently confirmed experimentally [7].

Under conditions of constant concentration the equations are appreciably simplified and can be solved analytically. This solution reveals a peculiar character of convective flows produced by the intensive transfer of solvent vapour in the gas phase. Since the diffusion flux in the liquid phase is negligible, Equation 1 takes the form

$$v = D^+ \frac{d\phi}{dx}. \qquad (15)$$

Thus, the velocity of the electrolyte flow must be such as to compensate for the migrative flow of non-discharging ions. Substituting Equation 15 into Equation 2 and neglecting the diffusive flux we obtain an equation for the potential:

$$(D^+ + D^-)c \frac{d^2\phi}{dx^2} = \nu_- Q(\phi). \qquad (16)$$

This is the usual equation in the macrokinetics of reactions in porous media. Boundary conditions for Equation 16 are defined by the current I at the polarized boundary $x = l$ of the electrode and by the zero current condition $d\phi/dx = 0$ at the opposite boundary, $x = 0$. Integrating Equation 16 we obtain the current density $i(x)$ in the cross-section x as a function of the potential ϕ in the same cross-section:

$$i(x) = -FJ^- = \frac{F(D^+ + D^-)c}{\nu_-}\frac{d\phi}{dx} = F\left[\frac{2c(D^+ + D^-)}{\nu_-}\int_{\phi^*}^{\phi} Q(\phi_1)d\phi_1\right]^{1/2} \qquad (17)$$

Integrating once again we obtain (in an implicit form) the potential distribution across the electrode $\phi(x)$:

$$x = \left|\int_{\phi^*}^{\phi}\left[\frac{2\nu_-}{c(D^+ + D^-)}\int_{\phi^*}^{\phi_1} Q(\phi_2)d\phi_2\right]^{-1/2} d\phi_1\right|. \qquad (18)$$

Assuming $x = l$ in Equation 17 we obtain the potential at the polarized boundary $\phi_0 = \phi(l)$ as a function of the current density $I = i(l) = F(D^+ + D^-)c(d\phi/dx)_{x=l}$:

$$I = F\left[\frac{2c(D^+ + D^-)}{\nu_-}\int_{\phi^*}^{\phi_0} Q(\phi)\,d\phi\right]^{1/2}. \qquad (19)$$

The potential ϕ^* at the back face of the electrode, in Equations 17–19, is found by solving the transcendental equation

$$l = \left|\int_{\phi^*}^{\phi_0}\left[\frac{2\nu_-}{c(D^+ + D^-)}\int_{\phi^*}^{\phi} Q(\phi_1)\,d\phi_1\right]^{-1/2} d\phi\right|. \qquad (20)$$

For a fast reaction, when the characteristic time $t_r = c/Q(\phi_0)$ is far smaller than the characteristic time of diffusion $t_d = l^2/(D_+ + D_-)$, the potential ϕ^* is close to the equilibrium value so that the reaction zone is localized at the polarized boundary (ohmic regime). For the opposite limiting case $t_r \gg t_d$, ϕ^* is close to ϕ_0 and the reaction proceeds uniformly over the whole thickness of the electrode (kinetic regime).

As follows from Equations 15 and 17, the flow velocity in the liquid phase is directly related to the current density in the given cross-section:

$$v(x) = \frac{D^+\nu_-}{F(D^+ + D^-)c}\, i(x). \tag{21}$$

The maximum flow velocity is observed at the polarized boundary $x = l$ and is equal to

$$v(l) = \frac{D^+\nu_-}{F(D^+ + D^-)}\, \frac{I}{c}. \tag{22}$$

This value is somewhat different from the estimate of Equation 10 obtained without regard for the convective currents caused by the transfer of solvent in the gas phase. However, the values (Equations 10 and 22) are close to one another for concentrated alkaline solutions in fuel cells and in water electrolysis units ($C_l/c \approx 5, D^+/D^- \approx 1/5$). The electrolyte flow is always directed against the current in an anodic reaction ($\nu_- < 0$) and parallel to the current in a cathodic reaction ($\nu_- > 0$). In hydrogen–oxygen fuel cells the electrolyte in the hydrogen electrode flows from the polarized boundary towards the back face while in the oxygen electrode the flow is in the opposite direction. Flow directions are reversed in the electrolyser.

The equation for the flow velocity in the gas phase is obtained by summing up Equations 3–5 taking due account of the constancy of pressure (Equation 13):

$$c_w \frac{dv}{dx} + C_g \frac{du}{dx} = (\nu_g + \nu_w)Q. \tag{23}$$

To solve this equation we have to impose the boundary conditions determining the flow of both the gas reagent and the solvent at the electrode boundary open for the gas. We shall assume that this boundary coincides with the back-face (non-polarized) boundary of the electrode $x = 0$:

$$J_w(0) \equiv (up_w - D_g dp_w/dx) + vc_w = (\alpha - \nu_w)I/F, \tag{24}$$

$$J_g(0) = up_g - D_g dp_g/dx = -\nu_g I/F. \tag{25}$$

Here we have taken into account the fact that the gas reagent flux is determined by the reaction stoichiometry. The deviation of the solvent flux from the stoichiometric value $-\nu_w I/F$ is accounted for by the parameter α which equals the dimensionless (with the scale I/F) outward solvent flux at the polarized boundary of the electrode. Summing up Equations 24 and 25, we obtain the boundary condition for the variable $vc_w + C_g u$:

$$(vc_w + uC_g)_{x=0} = (\alpha - \nu_w - \nu_g)I/F. \tag{26}$$

On integrating Equation 23 we obtain:

$$vc_w + uC_g = -F^{-1}\{[I - i(x)](\nu_g + \nu_w) - \alpha I\}. \tag{27}$$

In particular, the velocities of gas flow at the polarized and back-face sides of the electrode by virtue of Equation 21 are equal to,

$$\begin{aligned} u(0) &= (I/FC_g)(\alpha - \nu_g - \nu_w), \\ u(l) &= \frac{I}{FC_g}\left(\frac{D^+}{D^+ + D^-}\frac{c_w}{c} + \alpha\right). \end{aligned} \tag{28}$$

The Formulae 28 agree with the preliminary estimate Equation 10. Under different conditions the direction of the flow may either coincide with the electrolyte flow direction or be opposite to it. The velocity of the gas flow may also change sign so that the flow in different cross-sections of the electrode will be in opposite directions. In the next section we shall discuss the gas flow in more detail with reference to the hydrogen cell with a capillary membrane.

3. Mass transfer in a cell with capillary membrane

3.1. *Convective flows*

Consider a hydrogen–oxygen cell consisting of two porous electrodes separated by a porous membrane (Figs. 1 and 2). Equations of the reactions taking place at both electrodes are

$$1/2H_2O + OH^- = H_2O + e^-, \tag{29}$$

$$1/4O_2 + 1/2H_2O + e^- = OH^-.$$

The reactants (hydrogen and oxygen) are supplied through the outer faces of the corresponding electrodes; the reaction product (water) can be removed in the form of vapour on either side of the cell; 'through-transfer' of water across the cell is also possible if some additional amount of vapour is supplied to one electrode and removed from another.

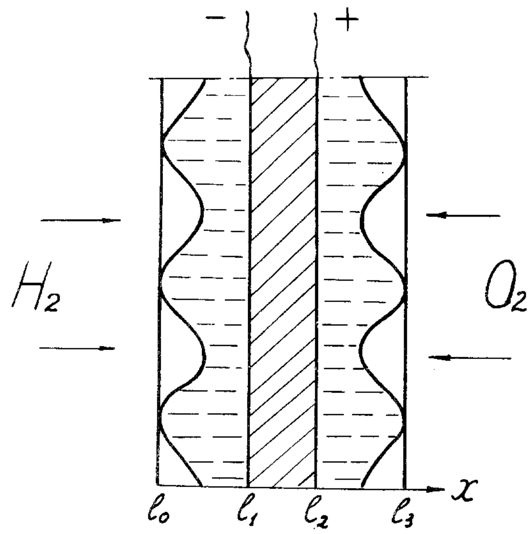

Fig. 1. Schematic presentation of hydrogen–oxygen fuel cell with capillary membrane and partially flooded electrodes.

Each electrode can be considered separately as in the preceding section. The system as a whole can be described by the Equations 1–6 and 13, if we index the parameters and the kinetic function Q in these equations ($i = 0, 1, 2$, for the membrane, anode and cathode, respectively). Since the membrane contains no gas phase and there is no electrochemical reaction here, Equations 1–3 with $Q = 0, q = 0$ are sufficient to describe it.

Let us investigate the values and the directions of the convective flows in the cell when the concentrations of reagents in each electrode can be assumed constant. The electrolyte flow velocities in the electrodes are given by Equation 21. The electrolyte flow rate in the membrane is directly related to the water flux from the hydrogen to the oxygen electrode:

$$v = \frac{\alpha I}{c_{\mathrm{w}} F} \tag{30}$$

When there is no through-transfer of water across the cell, the stoichiometric amount of water is transferred from the hydrogen to the oxygen electrode and enters into the reaction, while the excess water is vaporized from the outer boundary of the hydrogen electrode. In this case $\alpha = 1/2$. If the water vapour is additionally supplied to the oxygen electrode, α decreases and may even become negative. Since (Section 2.3) in both electrodes, liquid flows parallel to the potential gradient, in the usual situation ($\alpha > 0$) the directions of electrolyte flow in the membrane and electrodes are opposite to one another. The formulae for the flow velocity in the gas phase were already derived in the preceding section. These must be rewritten here for specific values of the stoichiometric coefficients for the fuel cell, ($\nu_1^{\mathrm{g}} = -1/2, \nu_1^{\mathrm{w}} = 1$, $\nu_2^{\mathrm{g}} = -1/4, \nu_2^{\mathrm{w}} = -1/2$) and the direction chosen for the x axis (from the hydrogen to the oxygen electrode, as shown in Fig. 2). Equation 23 and boundary condition 26 for the hydrogen electrode (anode) take the form

$$\frac{\mathrm{d}}{\mathrm{d}x}(vc_{\mathrm{w}} + uC_{\mathrm{g}}) = 1/2Q_1 \quad (0 \leqslant x \leqslant l_1) \tag{31}$$

$$vc_{\mathrm{w}} + uC_{\mathrm{g}} = (\alpha - 1/2)I/F \quad (x = 0). \tag{32}$$

Hence

$$vc_{\mathrm{w}} + uC_{\mathrm{g}} = F^{-1}\{-1/2[I - i(x)] + \alpha I\} \quad (0 \leqslant x \leqslant l_1). \tag{33}$$

The gas flow velocities at the outer and polarized boundaries of the electrode are equal to

$$u(0) = \frac{I(\alpha - 1/2)}{FC_{\mathrm{g}}}; \quad u(l_1) = \frac{I(\alpha + \chi_1)}{FC_{\mathrm{g}}}, \tag{34}$$

where $\chi_1 = D^+c_{\mathrm{w}}(0)/(D^+ + D^-)c(0)$. Corresponding formulae for the oxygen electrode are:

$$\frac{\mathrm{d}}{\mathrm{d}x}(vc_{\mathrm{w}} + uC_{\mathrm{g}}) = 3/4Q_2 \quad (l_2 \leqslant x \leqslant l_3), \tag{35}$$

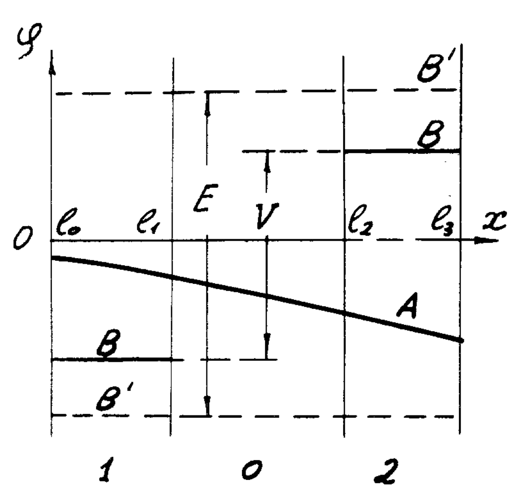

Fig. 2. Diagram of the potential distribution in the fuel cell. (0) membrane; (1) hydrogen electrode; (2) oxygen electrode. (A) electrolyte potential; (B) electrodes potentials in the operating cell and (B′) in the disconnected cell.

$$\varkappa c_{\mathrm{w}} + uC_{\mathrm{g}} = (\alpha - 3/4)I/F, \quad (x = l_3), \tag{36}$$

$$\varkappa c_{\mathrm{w}} + uC_{\mathrm{g}} = F^{-1}\{-3/4[I - i(x)] + \alpha I\} \quad (l_2 \leqslant x \leqslant l_3), \tag{37}$$

$$u(l_3) = \frac{I}{FC_{\mathrm{g}}}(\alpha - 3/4), \quad u(l_2) = \frac{I}{FC_{\mathrm{g}}}(\alpha + \chi_2), \tag{38}$$

where $\chi_2 = D^+c_{\mathrm{w}}(l_3)/(D^+ + D^-)c(l_3)$. The gas flow rates in the hydrogen and oxygen electrodes are schematically shown in Fig. 3. For $\alpha > 1/2$ the gas in the hydrogen electrode flows towards the membrane in a direction opposite to the electrolyte flow. For $1/2 > \alpha > -\chi_1$ the flow near the membrane retains its direction, but becomes outward-directed near the outer boundary. Finally, when a considerable amount of vapour is supplied from the oxygen electrode ($\alpha \leqslant -\chi_1$), in all electrode cross-sections the gas flows towards the outer boundary. For $3/4 > \alpha > -\chi_2$ (and, in particular, in the stoichiometric case $\alpha = 1/2$) in the oxygen electrode, the gas flows both from the outer boundary and from the membrane into the electrode. For $\alpha < -\chi_2$ the gas flows towards the membrane, and for $\alpha \geqslant 3/4$ it flows towards the outer boundary. These results are valid also for the hydrogen–oxygen electrolyser if the signs of all flows are reversed.

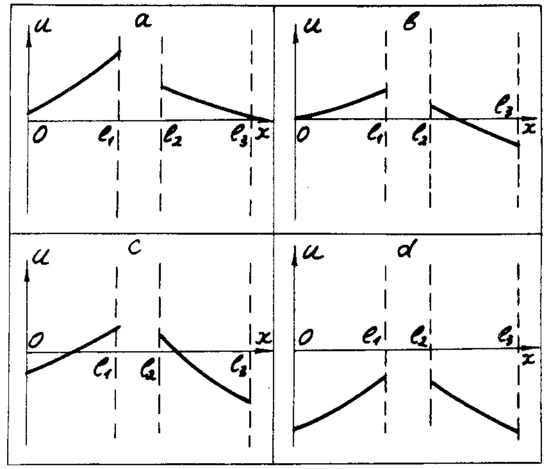

Fig. 3. Distribution of flow velocities in the gas phase (scheme): (a) $\alpha > 3/4$; (b) $3/4 > \alpha > 1/2$; (c) $1/2 > \alpha > -\chi$; (d) $\alpha < -\chi$.

3.2. *Concentration and potential distribution in the membrane*

Since $Q = 0$ in the membrane, Equation 2 can be integrated which yields the formula for the hydroxyl flux:

$$J^- = -D^-\frac{\mathrm{d}c}{\mathrm{d}x} + \varkappa c + D^-c\frac{\mathrm{d}\phi}{\mathrm{d}x} = -\frac{I}{F}. \tag{39}$$

Multiplying Equation 1 by D^- and Equation 39 by D^+ and summing them up we obtain, using Equation 30, an equation for the alkali concentration in the membrane,

$$\frac{\mathrm{d}c}{\mathrm{d}x} = \frac{I}{2FD^-}\left(1 + \frac{\alpha c}{t^+c_{\mathrm{w}}}\right) \tag{40}$$

where $t^+ = D^+/(D^+ + D^-)$. Neglecting both the dependence of the diffusion coefficients on the concentration and variations of water concentration (strictly speaking, this can be done only for dilute solutions), and integrating Equation 40 we obtain

$$c = \left(c_1 + \frac{t^+c_{\mathrm{w}}}{\alpha}\right)\exp\left[\frac{\alpha I(x - l_1)}{Fc_{\mathrm{w}}D^*}\right] - \frac{t^+c_{\mathrm{w}}}{\alpha}, \tag{41}$$

where $D^* = 2D^+D^-/(D^+ + D^-)$. If the membrane thickness $\delta = l_2 - l_1$ si much larger than the electrode thickness, then the major bulk of the electrolyte is contained in the membrane. The unknown concentration c_1 at the hydrogen electrode can then be found from the condition of constant total amount of alkali in the cell

$$\frac{1}{\delta}\int_{l_1}^{l_2} c(x)\,\mathrm{d}x = c_0 \tag{42}$$

where c_0 is the initial concentration at zero current. Substituting Equation 41 into Equation 42 and integrating we obtain

$$\frac{1}{\alpha y}\left(\frac{c_1}{c_0} + \frac{\chi}{\alpha}\right)(\mathrm{e}^{y\alpha} - 1) - \frac{\chi}{\alpha} = 1. \tag{43}$$

Here we have introduced dimensionless parameters $\chi = t^+c_{\mathrm{w}}/c_0$, $y = I\delta/FD^*c_{\mathrm{w}}$. From Equation 43 we obtain the concentrations at the hydrogen and oxygen electrodes c_1 and c_2:

$$\frac{c_1}{c_0} = \frac{y(\alpha + \chi)}{\mathrm{e}^{y\alpha} - 1} - \frac{\chi}{\alpha}; \quad \frac{c_2}{c_0} = \frac{y(\alpha + \chi)}{1 - \mathrm{e}^{-y\alpha}} - \frac{\chi}{\alpha}. \tag{44}$$

The dependence of the concentrations c_1 and c_2 on the parameter y (proportional to current) for

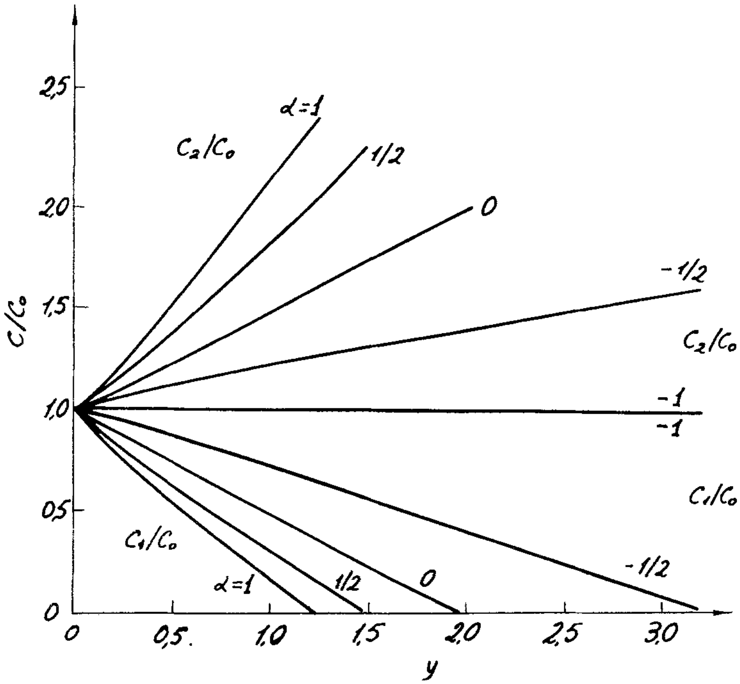

Fig. 4. Electrolyte concentrations at the membrane boundaries as functions of dimensionless current density for different values of the parameters α; $\chi = 1$.

$\chi = 1$ and for different values of α is plotted in Fig. 4.

For $\alpha > -\chi$ the concentration at the hydrogen electrode diminishes and that at the oxygen electrode increases with increasing current; the higher the value of α, the greater is the effect. At a certain value of current the concentration at the hydrogen electrode becomes zero. This current is limiting for this system. It is characteristic that the current limitation is independent of the electrode reaction kinetics and depends, most of all, on the nature of convective flows in the membrane. The water vapour inflow from the oxygen electrode reduces α and thus helps to attain higher values of current. For $\alpha = -\chi$ the concentration throughout the cell becomes constant and the limiting current becomes infinite. Finally, when the amount of vapour supplied from the oxygen electrode is so large that $\alpha < -\chi$, the concentration at the oxygen electrode goes below that at the hydrogen electrode, and any further reduction in α again decreases the limiting current.

The potential drop across the membrane can be found by integrating Equation 1

$$\Delta\phi = \frac{y\alpha}{2t^+} - \ln\frac{c_2}{c_1}. \tag{45}$$

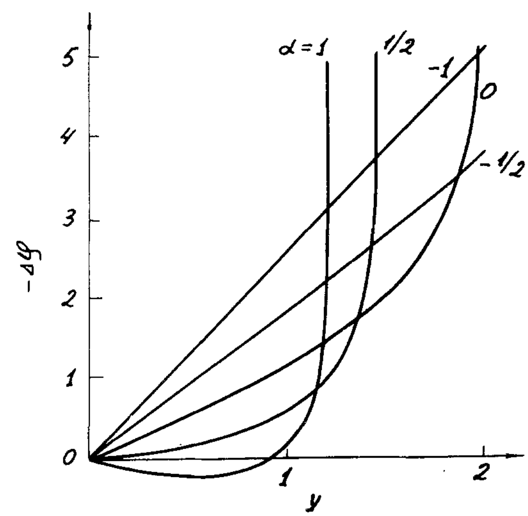

Fig. 5. Potential difference in the membrane as function of dimensionless current for different values of the parameter α ($\chi = 1$, $t^+ = 0{\cdot}2$).

The value of $\Delta\phi$ steeply increases as the current reaches its limiting value. The potential drop across the membrane decreases with decreasing current (Fig. 5).

These results are only qualitative since in actual processes, conducted with highly concentrated solutions, variation of the diffusion coefficients and of the water concentration across the membrane cannot be ignored. With variable c_w, D^+ and D^-, Equation 40 can be solved in quadratures, and the concentrations c_1 and c_2 can be found by nomograms [8], taking into account Equation 42. This does not change the qualitative behaviour of the above dependences. Accurate calculations with due regard for the concentration variation in the electrodes will be given in the next section. Calculations of the concentration and potential gradients in the membrane were reported earlier [8, 10–12].

For the usual values of the parameters the limiting current is about 10^{-1} A cm^2. Slightly higher currents and concentration gradients lower than the calculated values are observed in the experiments. It was explained [5, 9] by the presence of small gas inclusions in the membrane through which water transfer is supposed to proceed, accompanied, as is the case for the electrode, by successive evaporation and condensation. Intensification of the water transfer does not require that these gas inclusions form a connected system. If a correction is introduced to account for the water transfer via gas inclusions, then results are in good agreement with the experimental data [5, 9] (see Fig. 6).

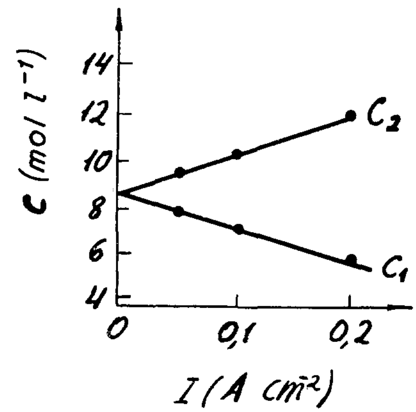

Fig. 6. Dependence of experimental (dotted) and calculated (solid curves) data on the electrolyte concentration difference in the membrane [11].

4. Steady-state regimes of hydrogen–oxygen fuel cell

4.1. *Transformation of equations*

In order to calculate the characteristics of a cell with thick electrodes, and high currents, when the concentration constancy condition is not satisfied, we have to solve the system of Equations 1–6 and 13 which can be transformed into a more convenient form by using the linear relationships between the flows of water, hydroxyl and gas reagent. Summing Equations 3 and 5 we obtain an equation for the water flux

$$\frac{dJ_w}{dx} = \frac{d}{dx}\left(\varkappa c_w + p_w u - D_g \frac{dp_w}{dx}\right) = \nu^w Q. \quad (46)$$

From Equations 2, 4 and 46 we obtain a linear relationship between the fluxes

$$\nu^w J^- - \nu^- J_w = \text{const}; \quad \nu^g J_w - \nu^w J_g = \text{const}. \quad (47)$$

To write these linear equations in an explicit form we shall use the values of fluxes at the outer boundaries of the cell ($x = 0, x = l_3$) and the stoichiometric coefficients for hydroxyl (ν_i^-), water (ν_i^w) and gas reactant (ν_i^g) in the hydrogen and oxygen electrode, as listed in the table below.

Electrode	H_2	O_2
i	1	2
ν_i^-	-1	$+1$
ν_i^w	$+1$	$-\frac{1}{2}$
ν_i^g	$-\frac{1}{2}$	$-\frac{1}{4}$
$\frac{F}{I}J_i^-$	0	0
$\frac{F}{I}J_i^w$	$\alpha-1$	$\alpha-\frac{1}{2}$
$\frac{F}{I}J_i^g$	$+\frac{1}{2}$	$-\frac{1}{4}$

Thus we obtain for the hydrogen electrode:

$$J^- = (\alpha-1)\frac{I}{F} - J_w; \quad J_g = \frac{\alpha}{2}\frac{I}{F} - 1/2 J_w \quad (48)$$

and for the oxygen electrode

$$J^- = (2\alpha-1)\frac{I}{F} - 2J_w; \quad J_g = -\frac{\alpha}{2}\frac{I}{F} + 1/2 J_w. \quad (49)$$

Using Equations 4 and 46 we can express the gas and electrolyte flow velocities via the fluxes J_g, J_w. Using the constancy condition for the total concentration in the gas phase Equation 13, as well as the equilibrium relation between the vapour pressure and the electrolyte concentration Equation 6, and introducing the notation $f_c = \mathrm{d}p_w/\mathrm{d}c$, we obtain

$$u = \frac{1}{C_g - p_w}\left(J_g - D_g f_c \frac{\mathrm{d}c}{\mathrm{d}x}\right), \tag{50}$$

$$w_w = J_w - \frac{p_w}{C_g - p_w} J_g + \frac{C_g}{C_g - p_w} D_g f_c \frac{\mathrm{d}c}{\mathrm{d}x}. \tag{51}$$

Substituting Equation 51 into Equation 1 and into the formula for the hydroxyl flux, expressing J^- and J_g via the water flux J_w by means of the linear relationships 48 and 49 and solving Equations 1 and 2 for the derivatives $\mathrm{d}c/\mathrm{d}x$, $\mathrm{d}\phi/\mathrm{d}x$, we obtain the system of equations for computations:

$$\Phi_0^{(i)}\frac{\mathrm{d}c}{\mathrm{d}x} = \Phi_1^{(i)};\quad \Phi_0^{(i)}\frac{\mathrm{d}\phi}{\mathrm{d}x} = \frac{\Phi_2}{c};\quad \frac{\mathrm{d}J^w}{\mathrm{d}x} = \nu_i^w Q^{(i)} \tag{52}$$

where

$$\Phi_0^{(i)} = 2D^- + \frac{D_i^g}{\chi}\frac{f_c}{1 - p_w/C_g} \tag{53}$$

$$\Phi_1^{(1)} = \left[1 + \frac{1}{\chi}\frac{C_g - p_w/2}{C_g - p_w}\right] J_w + \left[1 - \alpha - \frac{\alpha}{2\chi}\frac{p_w}{C_g - p_w}\right]\frac{I}{F}, \tag{54}$$

$$\Phi_1^{(2)} = \left[2 + \frac{1}{\chi}\frac{C_g - 3/2p_w}{C_g - p_w}\right] J_w + \left[1 - 2\alpha + \frac{\alpha}{2\chi}\frac{p_w}{C_g - p_w}\right]\frac{I}{F}, \tag{55}$$

$$\Phi_2^{(1)} = \left[\frac{1 + 2t^+}{\chi}\frac{C_g - p_w/2}{C_g - p_w} - \left(1 + \frac{1 - t^+}{\chi}\frac{D_g}{D^-}\frac{f_c}{1 - p_w/C_g}\right)\right] J_w - \left[(1-\alpha)\left(1 + \frac{1 - t^+}{\chi}\frac{D_g}{D^-}\frac{f_c}{1 - p_w/C_g}\right) + \frac{1 - 2t^+}{\chi}\frac{\alpha}{2}\frac{p_w}{C_g - p_w}\right]\frac{I}{F}, \tag{56}$$

$$\Phi_2^{(2)} = \left[\frac{1 - 2t^+}{\chi}\frac{C_g - 3/2p_w}{p_w} - 2\left(1 + \frac{1 - t^+}{\chi}\frac{D_g}{D^-}\frac{f_c}{1 - p_w/C_g}\right)\right] J_w + \left[\frac{1 - 2t^+}{2\chi}\frac{\alpha p_w}{C_g - p_w} - (1 - 2\alpha)\left(1 + \frac{1 - t^+}{\chi}\frac{D_g}{D^-}\frac{f_c}{1 - p_w/C_g}\right)\right]\frac{I}{F}. \tag{57}$$

The set of equations for the membrane (subscript $i = 0$) can also be written in the form (52) with the functions

$$\Phi_0^{(0)} = 2D^-;\quad \Phi_0^{(0)} = 1 + \frac{\alpha}{\chi};$$

$$\Phi_2^{(0)} = -1 + \frac{1 - 2t^+}{\chi}\alpha \tag{58}$$

and $Q^{(0)} = 0$. The rate of the electrode reactions is described by the kinetic functions $Q^{(1)}$, $Q^{(2)}$ which depend on the over-voltage at the active surface. If the solution potential in the disconnected cell is used as the reference point for the potential ϕ, then the over-voltage at the hydrogen electrode is $-\phi$, and that at the oxygen electrode is $\Delta V + \phi$, where ΔV is the total cell polarization, i.e. the difference between the e.m.f. E and the voltage across the operating cell V (see Fig. 2). In the simplest case of linear dependence of the electrochemical reaction rate on potential, the kinetic functions $Q^{(1)}$ and $Q^{(2)}$ take the form

$$Q^{(1)} = -k_1\phi;\quad Q^{(2)} = k_2(\Delta V + \phi). \tag{59}$$

To solve the set of equations (52) we must impose four boundary conditions (one more additional condition is required to determine the value ΔV). Water fluxes at the outer boundaries of the cell and at the membrane can be used as these boundary conditions;

$$J_w(0) = (\alpha - 1)I/F;\quad J_w(l_1) = \alpha I/F;$$

$$J_w(l_3) = (\alpha - \tfrac{1}{2})I/F \tag{60}$$

and the condition of the constant amount of alkali in the cell;

$$\omega\left[\int_0^{l_1} c\,\mathrm{d}x + \int_{l_2}^{l_3} c\,\mathrm{d}x\right] + \int_{l_1}^{l_2} c\,\mathrm{d}x = \text{const}$$

$$= c_0[(l_2 - l_1) + \omega_0(l_3 - l_2 + l_1)], \tag{61}$$

where ω_0, c_0 are the initial moisture content and alkali concentration in the disconnected cell. The above theory is applicable also to the electrolyser provided we use appropriate kinetic relationships and stoichiometric coefficients.

4.2. *Cell characteristics for fixed moisture content*

The system of equations (52) with the boundary conditions (60), (61) was solved with the help of a computer [12]. Current density I, average electrolyte concentration c_0, thickness of hydrogen, oxygen electrodes and membrane ($\delta_1 = l_1$; $\delta_0 = l_2 - l_1$; $\delta_2 = l_3 - l_2$), temperature T, external pressure Π, and the parameter α determined by the outward water flows were taken as the parameters. The following set of parameters was used as the basic set for calculation: $I = 0{\cdot}1$ A cm^{-2}, $c_0 = 10^{-2}$ mol cm^{-3}, $\delta_1 = \delta_2 = 0{\cdot}03$ cm, $\delta_0 = 0{\cdot}05$ cm; $T = 90°$ C, $\Pi = 1$ atm, $\alpha = 0{\cdot}5$. In all computations we started with the basic set and varied one parameter while the others were kept constant.

The following values of the parameters were also assumed: $k_1 = 100\ \mathrm{s}^{-1}$, $k_2 = 1\ \mathrm{s}^{-1}$; liquid content in the electrodes $\omega = 0{\cdot}5$; diffusion retardation factors $\epsilon_1^g = \epsilon_2^g = \epsilon_1^l = \epsilon_2^l = 0{\cdot}1$ in the electrodes and $\epsilon_0^l = 0{\cdot}33$ in the membrane.

Dependences of the solution density, ion transport coefficients, water and electrolyte activities and the saturated vapour pressure on the electrolyte concentration and on temperature [13–15] were used in the calculations. Figs. 7 and 8 show the distributions of dimensionless concentration and potential across the cell, calculated for $c_0 = 7$ mol/l^{-1} and $\alpha = 1/2$. It is observed that the concentration Δc and potential $\Delta\phi$ gradients increase with I. As the current approaches its limiting value, concentration gradients at the electrodes also become appreciable. Corresponding gradients in the electrodes are much lower than those in the membrane which shows the effectiveness of the concentration equalization due to water transfer via the gas phase.

Concentration gradients at the hydrogen electrode are lower than those at the oxygen electrode due to the higher diffusion rate of hydrogen. It is typical that the electrolyte concentration at the hydrogen electrode passes through a minimum. This is caused by different directions of water fluxes in different parts of the hydrogen electrode. For $\alpha = 1/2$ water is transferred from the centre of the hydrogen electrode towards its outer boundary and also to the membrane; as water is mostly transported via the gas phase, the water concentration must diminish in these directions while the electrolyte concentration must rise accordingly. Minimum concentration is located close to the membrane surface. Since the reaction at the

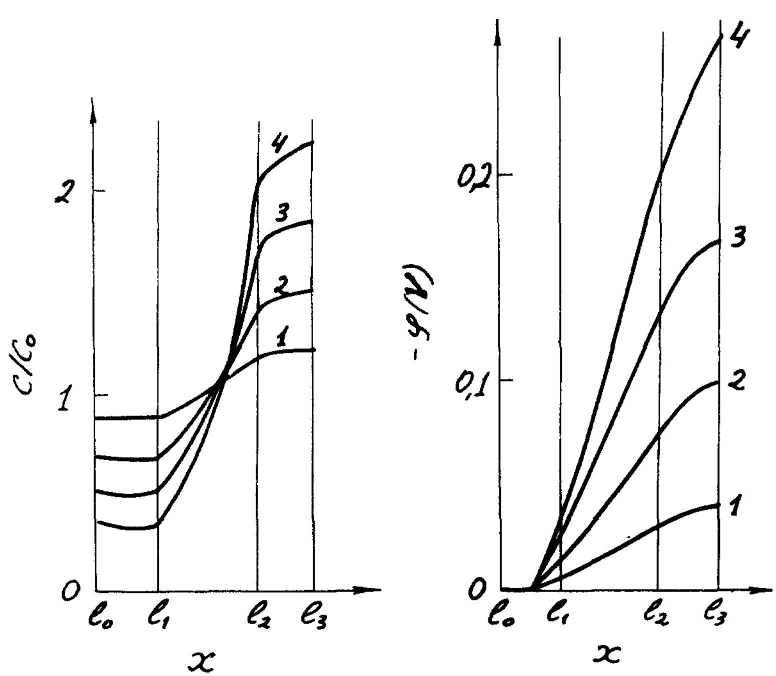

Figs. 7 and 8. Concentration and potential distributions over the cell thickness: (1) $I = 0{\cdot}1$; (2) $I = 0{\cdot}25$; (3) $I = 0{\cdot}4$; (4) $I = 0{\cdot}55$ A cm^{-2}.

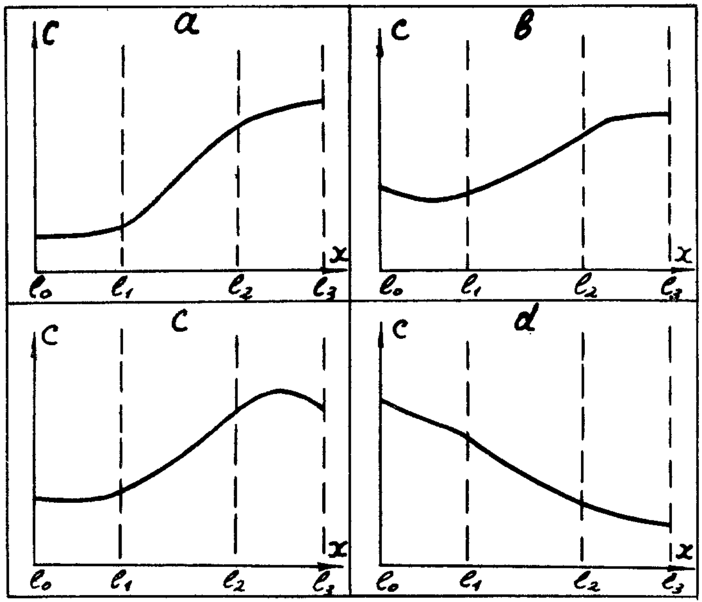

Fig. 9. Concentration distribution across the cell (scheme):

(a) $\alpha > \dfrac{C_g - p_w/2}{C_g - p_w}$;

(b) $\dfrac{C_g - p_w/2}{C_g - p_w} > \alpha > 1/2 - \dfrac{p_w}{C_g - p_w}$;

(c) $1/2 - \dfrac{p_w}{C_g - p_w} > \alpha > -\chi$;

(d) $\alpha < -\chi$.

hydrogen electrode is quite fast, the reaction zone is located close to the membrane where polarization is a minimum. Water flows out in different directions from the reaction zone, so that the concentration minimum is located within this zone.

Substituting the expressions for water fluxes at the hydrogen electrode boundaries into the function, Equation 54, we can easily see that the electrolyte concentration minimum inside the hydrogen electrode exists within the range of α variation, from $-\chi$ to $(C_g - p_w/2)/(C_g - p_w)$. This last value exceeds unity so that the steady increase of electrolyte concentration from the outer boundary of the hydrogen electrode towards the membrane is only possible in non-real cases when not only all reaction-produced water is removed from the oxygen electrode (this corresponds to $\alpha = 1$) but also there is a through-flow of water vapour from the hydrogen to the oxygen electrode. Steady reduction of concentration is possible if $\alpha \leqslant -\chi$, i.e. when there is a sufficiently strong through-flow of water from the oxygen to the hydrogen electrode. As shown in the preceding section, the electrolyte concentration in the membrane under these conditions also diminishes from the hydrogen to oxygen electrode. Similar investigation of the function, Equation 55 shows that the electrolyte concentration in the oxygen electrode steadily increases when $\alpha \geqslant 1/2 - p_w/(C_g - p_w)$ in the direction from the membrane to the outer boundary, passes through a minimum when $-\chi < \alpha < 1/2 - p_w/(C_g - p_w)$, and decreases when $\alpha \leqslant -\chi$. Concentration distribution in the cell for various values of α is schematically shown in Fig. 9.

The distribution of the electrolyte and gas flow velocities remains qualitatively the same as in the case of constant concentration discussed in the preceding section (see Fig. 3). Quantitative dependences for the current densities $I = 0{\cdot}1$ A cm^{-2} and $0{\cdot}25$ A cm^{-2} are shown in Fig. 10 for $\alpha = 1/2$. The distribution of dimensionless values $v' = vFc_w/I$ and $u' = uFC_g/I$ varies only slightly as the current increases; thus the absolute values of velocities in both phases rise approximately proportional to the current.

Figs. 11–24 show the calculated dependences of c_j, ϕ, ΔV, $W = \Delta V + \Delta E = E_0 - V$ on the following parameters: I, c_0, δ_0, δ_1, δ_2†. The value ΔV characterizes the total potential drop in the cell. Fig. 11 shows that the potential drop in the membrane $(\phi_1 - \phi_2)$ and the value ΔV increase as α decreases, i.e. as water transport from the oxygen to the hydrogen electrode is intensified. This can be explained by the fact that a reduction in the diffusion component of the hydroxyl flux (this happens when α decreases) is accompanied by

† Numbers 0, 1, 2, 3 on the curves show that the corresponding potentials and concentrations refer to the points $x = 0, x = l_1, x = l_2, x = l_3$ (see Fig. 2).

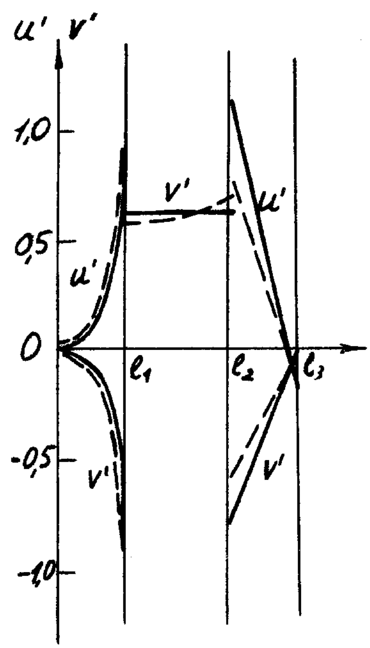

Fig. 10. Distribution of dimensionless velocities in the electrolyte $v' = vFc_0/I$ and gas $u' = uFC_g/I$ across the cell. Solid curves: $I = 0{\cdot}1$, dotted curves: $I = 0{\cdot}25$ A cm^{-2}.

an increase in its migration component, since their sum, equal to the total hydroxyl flux, in independent of α.

It may appear that an increase in ΔV due to a decrease in α during the intensification of mass transfer in the fuel cell must result in reduced voltage across this element $V = E - \Delta V$. This, however, is not the case since not only ΔV but also the e.m.f. E of the cell depend on component concentrations. The change in the e.m.f. $\Delta E = E_0 - E$ corresponds to the voltage of the concentration cell connected opposite to the chemical cell. This can be calculated by the usual thermodynamical formulae, using average concentrations of the electrolyte at the hydrogen and oxygen electrodes, (this is justified by negligible variations of these concentrations).

After this correction is introduced we find that due to increased transfer of water from the hydrogen to the oxygen electrode the cell voltage rises despite an increase in the cell polarization ΔV. Figs. 13, 15 and 21 show that the sum $\Delta V + \Delta E$ increases with the current and the membrane thickness δ_0 and is practically independent of c_0.

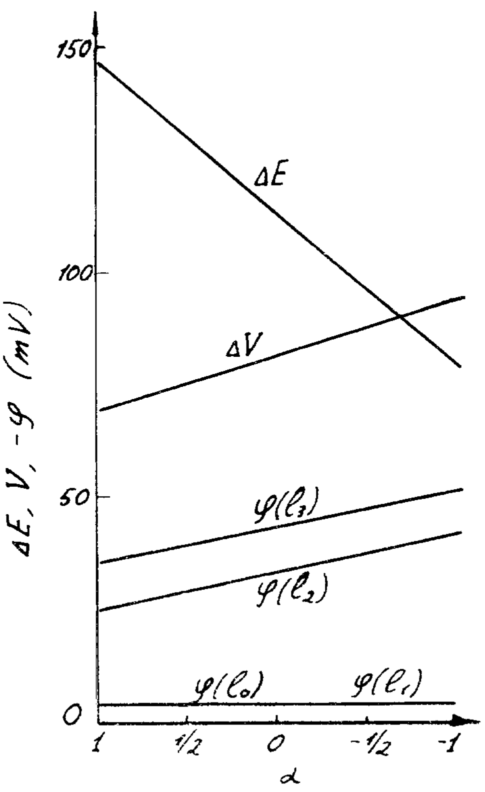

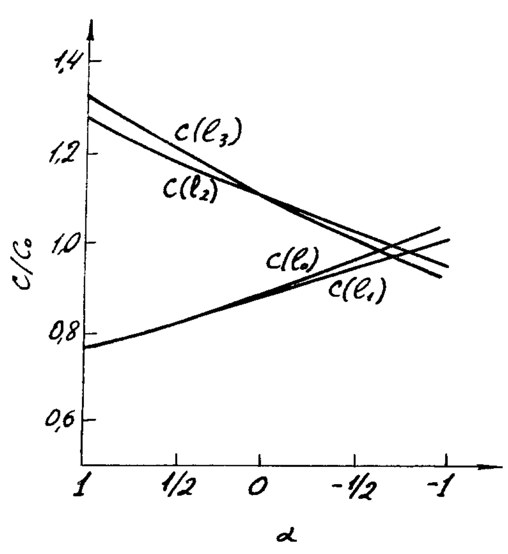

Figs. 11 and 12. Potentials and concentrations as functions of the parameter α.

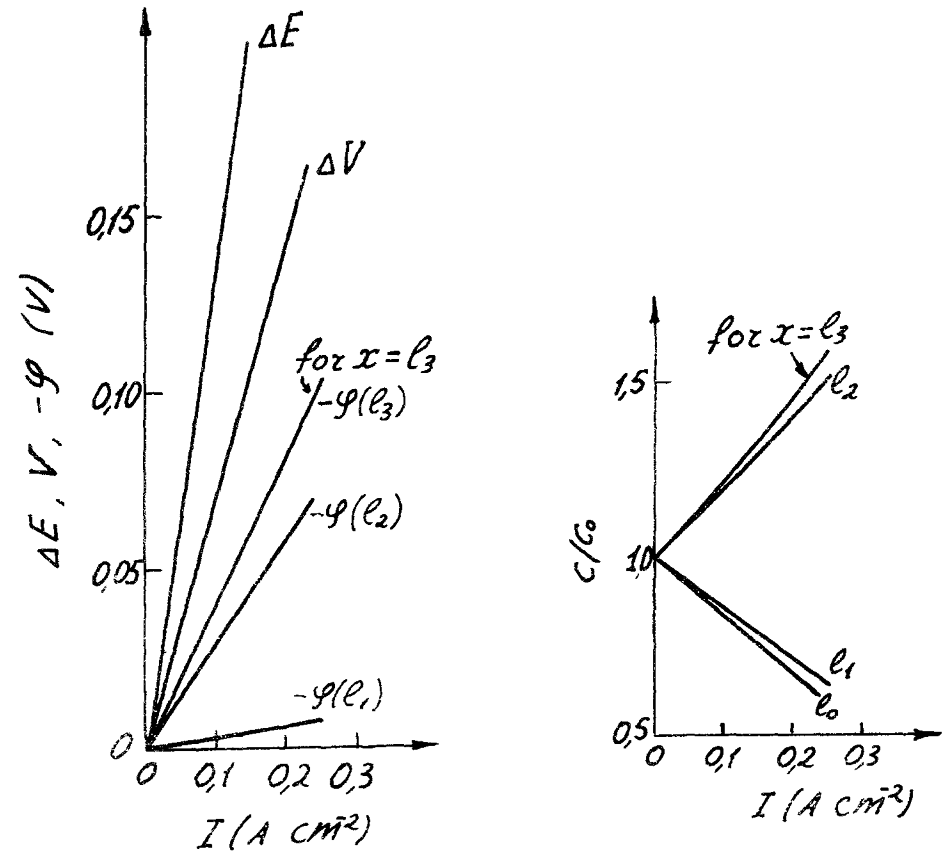

Figs. 13 and 14. Potentials and concentrations as functions of the current density.

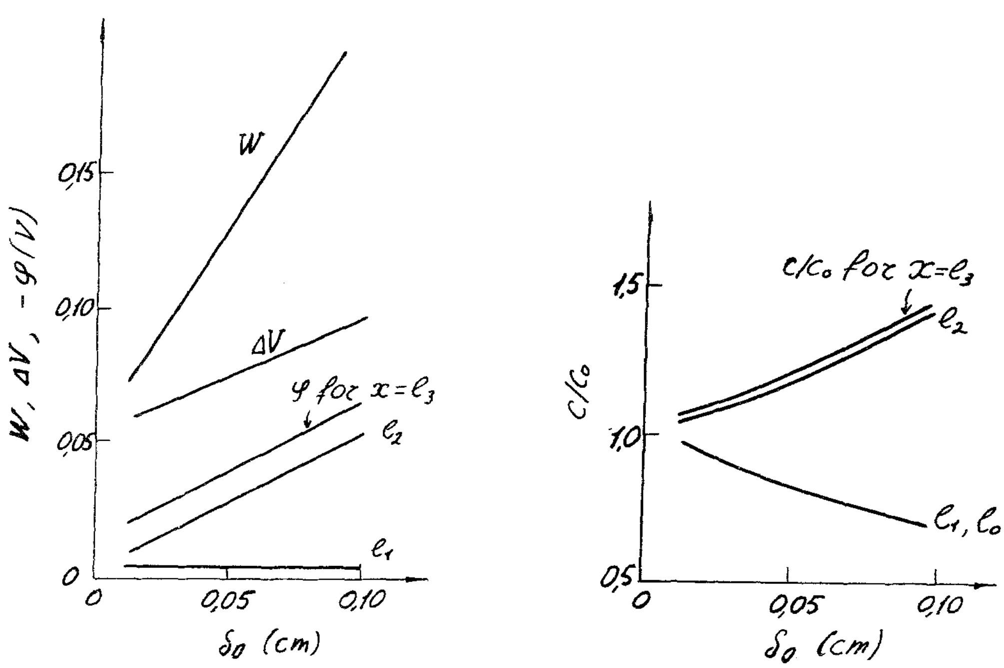

Figs. 15 and 16. Potentials and concentrations as functions of the membrane thickness.

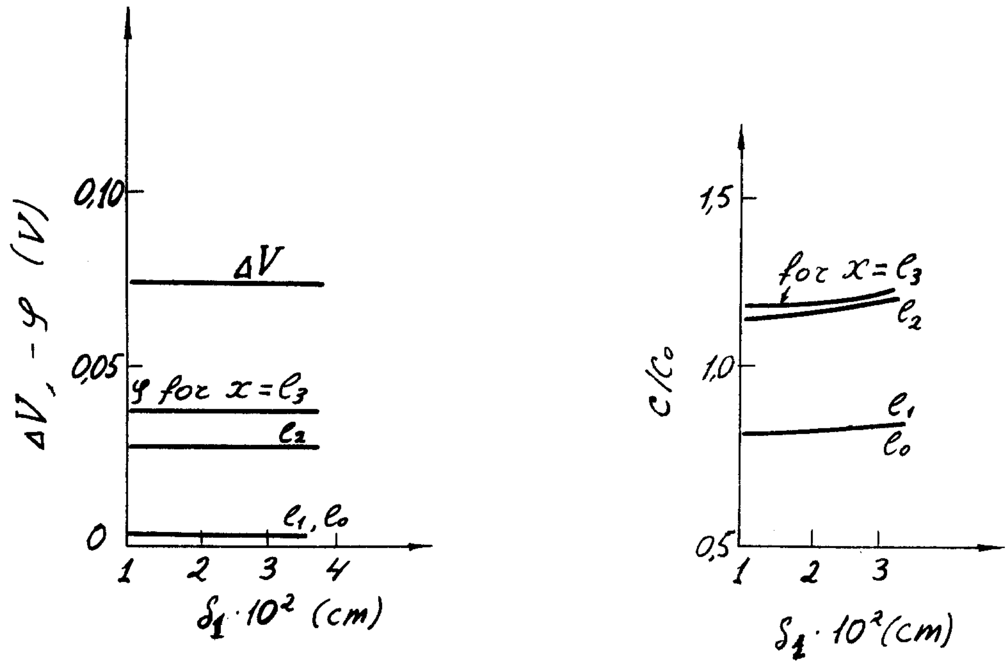

Figs. 17 and 18. Potentials and concentrations as functions of the hydrogen electrode thickness.

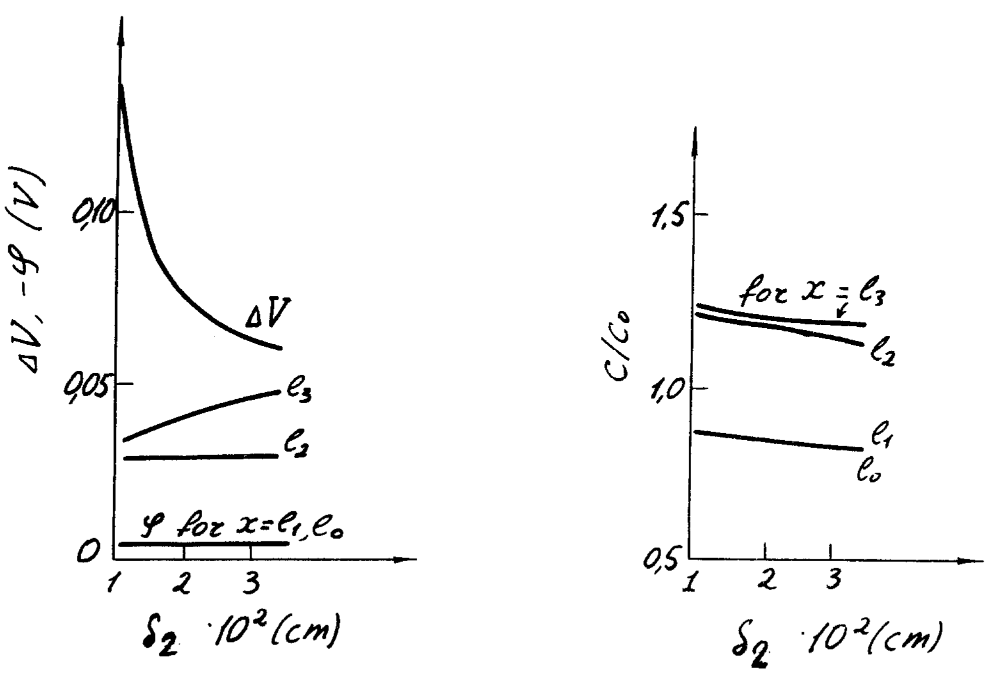

Figs. 19 and 20. Potentials and concentrations as functions of the oxygen electrode thickness.

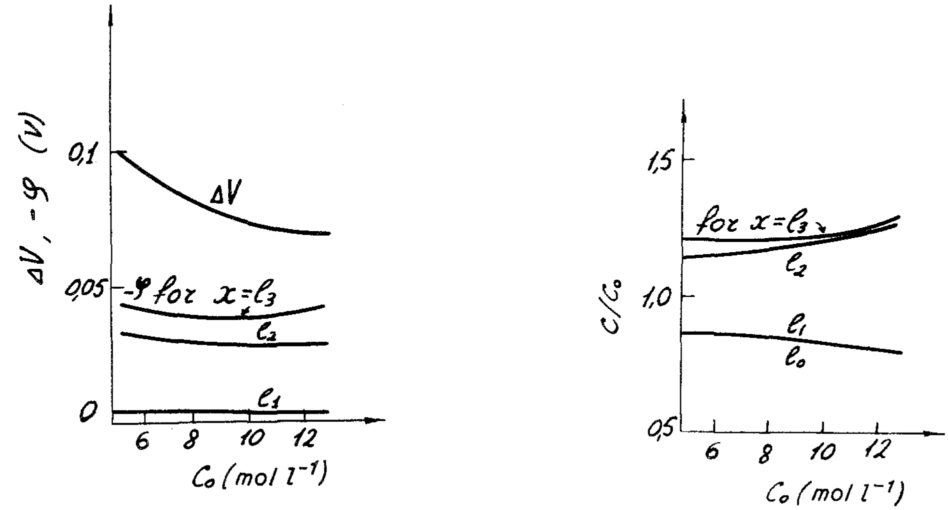

Figs. 21 and 22. Potentials and concentrations as functions of the initial electrolyte concentration.

Fig. 22 demonstrates that the increase in the average concentration c_0 results in an increased concentration gradient mostly due to the concentration-induced reduction of D^+ and D^-. The rise in δ_0 and I results in almost proportional increase in both the concentration gradient and ΔV (Figs. 13–16). It is seen in Fig. 11 that reduction of α leads to a proportional increase in ΔV practically only at the expense of the membrane, since the potential field in the electrodes remains virtually unchanged.

Figs. 17 and 18 show the almost complete non-dependence of all characteristics on the thickness δ_1 of the hydrogen electrode; this is due to the fact that the characteristic depth of reaction penetration into the hydrogen electrode is much smaller than its thickness because of the high value of k_1. The penetration depth in the oxygen electrode is by an order of magnitude higher, so that it is commensurable with the electrode thickness δ_2. Therefore, the increase of δ_2 increases the concentration $(c_3 - c_2)$ and the potential $(\phi_2 - \phi_3)$ drops and reduces ΔV due to the decreased polarization of the oxygen electrode (Figs. 19 and 20).

As can be seen in Figs. 23 and 24, the concentration and potential gradients in the cell decrease with increasing temperature, as a result of more intensive transport due to increased water vapour

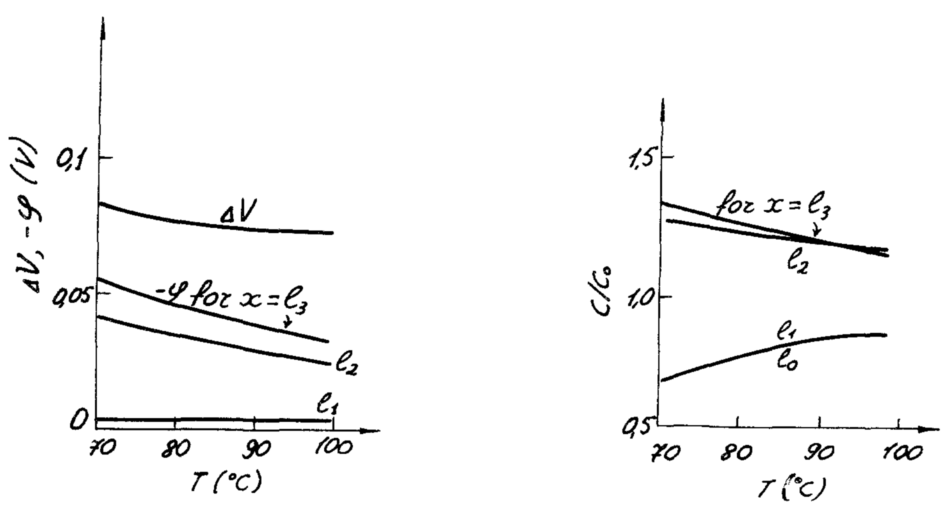

Figs. 23 and 24. Potentials and concentrations as functions of temperature.

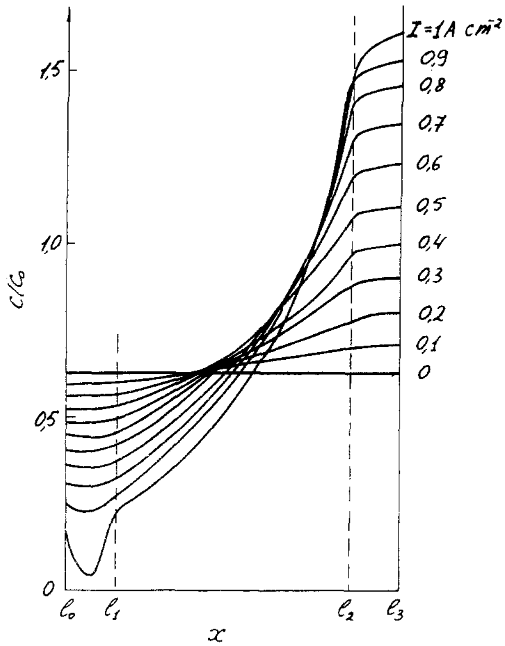

Fig. 25. Concentration distribution across the cell for different current densities ($\beta = 1$, $\omega_0 = 0{\cdot}6$).

pressure. Calculations also show that the potential and concentration distributions remain practically unchanged as the total pressure varies in the range from 0·5 to 3 atm.

4.3. *Problems of self-regulation of a fuel cell*

This section continues the investigation of the problems of the self-regulation of the supply and removal of water vapour which was initiated in earlier papers [5, 16, 17].

In the operation of a fuel cell the water vapour pressure in the gas chamber near the hydrogen electrode is usually constantly maintained. When water vapour is supplied from the oxygen elect trode, the constant water vapour pressure is maintained in two gas chambers near each electrode. In both cases the liquid content in the electrodes is so adjusted during the cell operation that the evolution of water due to the reaction is compensated by its removal, so that the cell operates in a steady state. If the moisture exchange is unidirectional, i.e. proceeds from the hydrogen electrode only, then $\alpha = 1/2$ always. With the bi-directional moisture exchange, when vaporization and condensation proceed at the outer boundaries of both electrodes, there is an additional flow of water through the cell; this flow corresponds to the steady-state process at given pressures of water vapour in both gas chambers. Both the liquid content and the water flux change as the current varies. Since current generation is not possible at excessive drying nor, on the contrary, at flooding of the electrodes, a problem of practical interest is how wide is the current range in which the steady-state operation of the cell is still possible with liquid contents remaining within acceptable limits.

The increased current increases the electrolyte concentration gradient (mostly due to an increased concentration gradient in the membrane). At $\alpha = 1/2$, when the water exchange takes place only

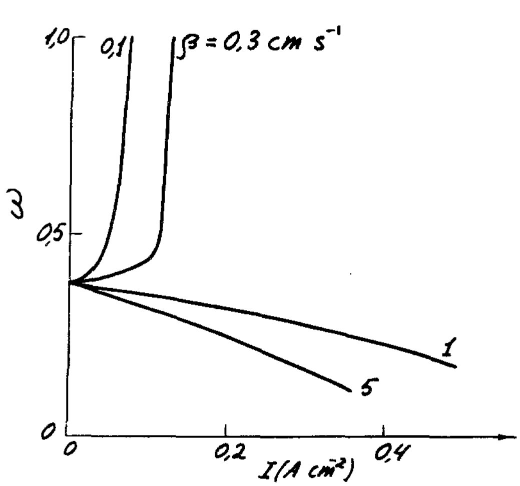

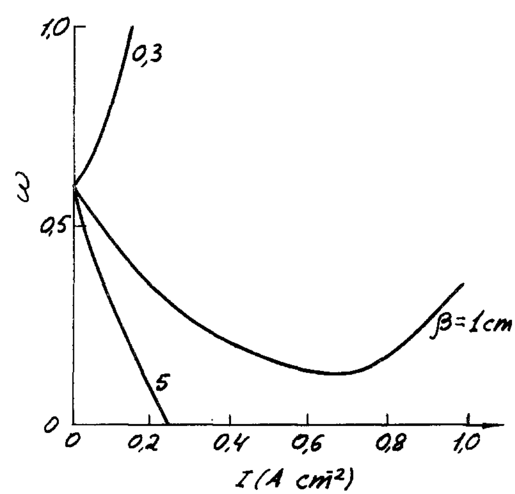

Figs. 26 and 27 Liquid content as function of current for different values of the mass transfer coefficient β.

at the hydrogen electrode, the electrolyte concentration at the hydrogen electrode decreases as the current increases; correspondingly, both the saturated vapour pressure and the water removal rate also increase. Thus the cell exhibits self-regulatory characteristics; the faster the evolution of water, the faster is its removal [16]. This self-regulation is, however, not ideal. For a small coefficient of mass transfer from the electrode surface to the gas chamber the intensification of water removal due to the increased concentration gradient is not sufficient to compensate for the intensified water evolution, so that the cell is flooded as the current increases. This flooding decreases the electrolyte concentration and thus is conducive to the intensification of water removal. However, the steady-state moisture content gradually increases as the current rises, and finally exceeds the acceptable limiting level. At a high mass transfer coefficient we must observe a reversed situation: a small increase in the concentration gradient will lead to such a considerable intensification of water removal that the electrodes will gradually dry up as the current increases. As was shown by Volfkovich *et al.* [17] the most effective self-regulation must be expected at certain intermediate values of the mass trans coefficient.

An additional possibility of self-regulation not only of the liquid content but also of the water flux, and hence of the concentration gradient in the cell, appears in the systems with bi-directional water exchange. In the usual case, when the electrolyte concentration decrease in the direction from the oxygen towards the hydrogen electrode, the increased concentration difference, produced by the rise of current, results in intensified water transfer from the oxygen gas chamber to the oxygen electrode, and from the hydrogen electrode to the hydrogen gas chamber; therefore, the parameter α decreases. However, smaller α values correspond to lower concentration gradients; therefore, these gradients are affected by the current increase much less than in the case of unidirectional moisture exchange. The current increase both in the bi-directional and unidirectional moisture exchanges can lead under different conditions to drying and also flooding of the electrodes. As the difference between water vapour pressures in both gas chambers decreases, the range of the most effective self-regulation shifts towards higher values of the mass transfer coefficients. To solve quantitatively the problem of the external water transfer self-regulation we have to integrate the system of Equations 52 with the additional boundary conditions which make it possible to calculate the values of ω and α. The balance of water fluxes at the outer boundaries of the hydrogen and oxygen electrodes, with due regard for the Stefan flow of the vapour–gas mixture, gives the boundary conditions

$$(\alpha-1)\frac{I}{F} = \frac{\beta_1 C_g}{\gamma_1}\ln\frac{1-\gamma_1 p_w/C_g}{1-\gamma_1 p_w^{(1)}/C_g} \qquad (62)$$

$$(\alpha-1/2)\frac{I}{F} = \frac{\beta_2 C_g}{\gamma_2}\ln\frac{1-\beta_2 p_w^{(2)}/C_g}{1-\gamma_2 p_w/C_g}. \qquad (63)$$

Here β_1 and β_2 are mass transfer coefficients from the hydrogen and oxygen electrodes, respectively, and $p_w^{(1)}$ and $p_w^{(2)}$ are water vapour pressures in the respective gas chambers. The values on the left-hand sides of Equations 62 and 63 represent the water fluxes at the outer boundaries of the hydrogen and oxygen electrodes which correspond to the steady-state process at a given current density I and at certain values of the parameter α.

The right-hand sides of these equations contain the expressions for the water transfer rate from the electrode surface to the bulk of the gas chamber under Stefan flow [18]. Coefficients γ_1 and γ_2 are equal to the number of moles of the gas mixture transferred with one mole of water. According to the stoichiometry of the electrode reactions:

$$\gamma_1 = \frac{\alpha-1/2}{\alpha-1}; \quad \gamma_2 = \frac{\alpha-3/4}{\alpha-1/2}. \qquad (64)$$

The cell characteristics for unidirectional moisture transfer are obtained from Equation 52 under the boundary conditions 60–62. In this case $\alpha = 1/2$, and the additional boundary condition, 62, serves to determine the moisture content in the electrodes ω. Since at $\alpha = 1/2$ we have $\gamma_1 = 0$, in this case this boundary condition reduces to

$$1/2F = \beta_1(p_w - p_w^{(1)}). \qquad (65)$$

To find the value of α another boundary condition, 63, is required for bi-directional water exchange.

Some results of calculations for $\alpha = 1/2$ are plotted in Figs. 25–28. In these calculations we

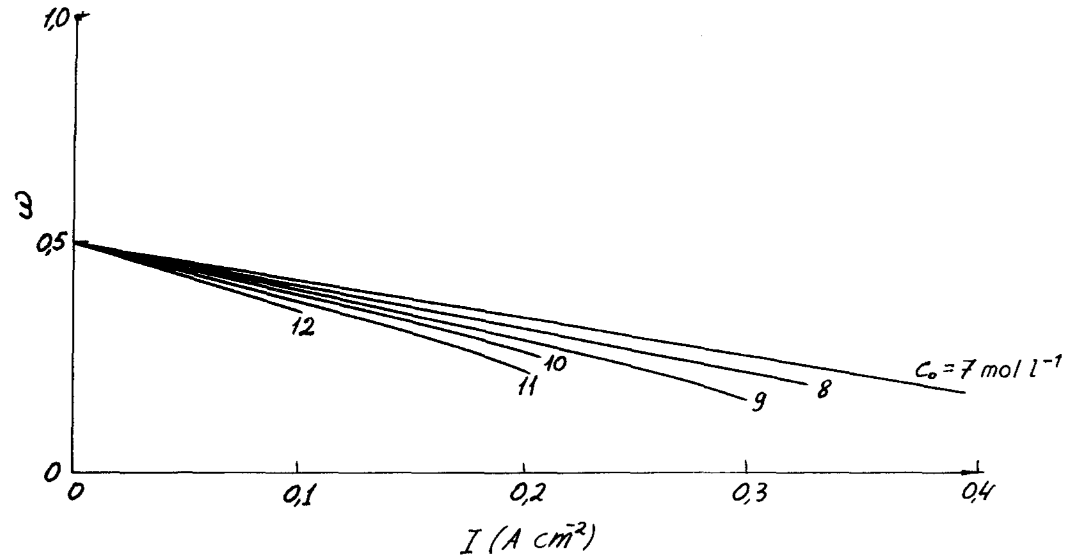

Fig. 28. Liquid content as function of current density at various initial electrolyte concentrations.

took into account the dependence of the effective diffusion coefficients in the liquid and gas phases on the liquid content $[D_g \sim (1-\omega)^2; D^{\pm} \sim \omega^2]$. The kinetics of the electrode reactions hardly affects water transfer in the cell (which play decisive roles in the problem of self-regulation). Thus in calculations we can assume that evolution of water is either located at a small segment of the electrode or is uniformly distributed throughout the whole bulk of the electrode. The difference between these two versions is revealed only in some modification of the electrolyte concentration distribution in the electrodes. Since the concentration difference in the electrodes is much lower than that in the membrane, these small changes practically do not affect the calculated value of the moisture content.

Fig. 25 shows the variation of the concentration distribution in the cell with the current. The qualitative characteristics of the distribution, discussed above in 4.2., remain unchanged despite the fact that, in contrast to the foregoing results, variation of current is accompanied by changes in the electrode liquid content in this case. Figs. 26 and 27 show the character of the current-induced liquid content variation for various values of the mass transfer coefficient β. Both figures differ in the initial liquid content of the electrodes (or, in other words, in the total amount of alkali in the cell). The results of the calculations corroborate the results that the cell is flooded at low mass transfer coefficients and that it dries at high values of these coefficients when the current is increased [17]. The curve in Fig. 27, corresponding to $\beta = 1$ cm s^{-1}, is of special interest. Here. an increase in current first reduces and then increases the liquid content. Non-monotonous behaviour of ω, Equation 1, is really observed at intermediate values of the mass transfer coefficient optimal from the standpoint of self-regulation; this leads to widening of the current range in which the fuel cell operation is stable. Fig. 28 illustrates a certain deterioration in the self-regulation characteristics when the initial alkali concentration is increased as revealed by a rapid drying of the cell with increasing current. Calculations by this method enable us to estimate in a similar way the effects of various parameters, determining both the dependence of the design and the operation mode of a fuel cell, on its self-regulation characteristics. The calculation principles are applicable both to a fuel cell and to an electrolyser in which water is supplied and removed as vapour.

References

[1] Yu. A. Chizmadjev, V. S. Markin, M. R. Tarasevich and Yu. G. Chirkov, 'Macrokinetics of processes in porous media', 'Nauka', Moscow, 1971.

[2] L. M. Pismen and S. I. Kuchanov, *Dokl. AN SSSR*, **203** (1972) 163.

[3] N. S. Lidorenko and V. A. Onishchuk, *Dokl. AN SSSR*, **201** (1971) 1339.
[4] *Idem*, *Elektrokhimiya*, 8 (1972) 672.
[5] V. S. Bagotzky and Yu. M. Volfkovich, *J. Appl. Electrochem.* **2** (1972) 315.
[6] O. S. Ksenjek, E. A. Kalinovsky and E. L. Baskin, *Zhur. fiz. Khim.* **37** (1964) 1045.
[7] B. G. K. Muzthy, D. Gidaspow and D. Ray, *A.I. Ch. E.J.* **19** (1973) 31.
[8] V. S. Bagotzky, Yu. M. Volfkovich, L. M. Pismen, S. I. Kuchanov, *Electrokhimiya*, 7 (1972) 1013.
[9] I. A. Kukushkina, G. V. Steinberg, Yu. M. Volfkovich and V. S. Bagotzky, *ibid*, 8 (1972) 1451.
[10] R. Kh. Burshtein, A. G. Pshenichnikov, M. R. Tarasevich, Yu. A. Chizmadjev and Yu. G. Chirkov, *ibid*, **8** (1972) 1688; **9**, 107 (1973) 101.
[11] O. S. Ksenjek, E. A. Kalinovsky, B. G. Grishayenkov, B. M. Shenbel and V. A. Peredkov, *ibid*, **9** (1973) 358, 647.
[12] L. M. Pismen, S. I. Kuchanov, Yu. M. Volfkovich, R. P. Goryachev and V. S. Bagotzky, *ibid*, **9** (1973) 1264.
[13] V. Yu. Yushkevich, I. N. Maksimova and V. T. Bullan, *ibid*, **3** (1967) 1491.
[14] H. S. Harned, B. B. Owen, 'The Physical Chemistry of Electrolytic Solutions', Reinhold, New York, 1964.
[15] International Critical Tables, **3** p. 373.
[16] V. S. Bagotzky *et al.*, *Inzh. fiz. zhur.*, **21** (1971) 627.
[17] Yu. M. Volfkovich, V. E. Sosenkin and V. S. Bagotzky, *ibid* **23** (1972) 618.
[18] D. A. Frank-Kamenetsky, 'Diffusion and heat transfer in chemical kinetics', 'Nauka', Moscow, 1967.